LIMNOLOGY and OCEANOGRAPHY

ASLO

Limnol. Oceanogr. 71, 2026, e70459

doi: 10.1002/lno.70459

RESEARCH ARTICLE

Sediment transport outweighs flow resumption mode as a driver of river carbon and nitrogen dynamics in a temporary stream

José Schreckinger,[1,2] **Matthias Koschorreck**,[3] **Lediane Marcon-Henge**,[1,4] **Mario Brauns**,[5] **Simon Rudolph**,[1] **Catalina Osorio-Pelaez**,[1] **Travis Meador**,[6,7] **Clara Mendoza-Lera**[1*]

[1]Institute of Environmental Sciences, University of Kaiserslautern-Landau (RPTU), Landau, Germany; [2]Research Unit Biodiversity and Conservation Biology, Swiss Federal Research Institute for Forest, Snow and Landscape Research (WSL), Birmensdorf, Switzerland; [3]Department Lake Research, Helmholtz Centre for Environmental Research, Magdeburg, Germany; [4]Institute of Bio- and Geosciences: Agrosphere (IBG-3), Research Centre Jülich, Jülich, Germany; [5]Department of River Ecology, Helmholtz Centre for Environmental Research-UFZ, Magdeburg, Germany; [6]Institute of Soil Biology and Biogeochemistry, Biology Center CAS, České Budějovice, Czech Republic; [7]Faculty of Science, University of South Bohemia, České Budějovice, Czech Republic

Abstract

Although transitions from dry-to-flowing conditions in non-perennial rivers are recognized as biogeochemical hot moments, the drivers modulating these hot moments remain poorly understood. We identify two main drivers of importance for biogeochemical processes during flow resumption: the dry-to-flow mode, referring to how flow is re-established, and whether resumption leads to sediment transport. Using experimental flumes, we examined how instant and gradual surface flows (the latter preceded by 6-h inundation), with varying sediment transport rates, affect streambed biogeochemistry. Over 24 h, we measured carbon dioxide (CO_2), methane (CH_4), and nitrous oxide (N_2O) fluxes and porewater concentrations, and analyzed the temporal dynamics of CO_2 fluxes and dissolved oxygen. Additionally, we added isotope-labeled nitrate to trace denitrification through changes in nitrogen gas isotope ratios ($\delta^{15}N\text{-}N_2$) and determined the uptake and release rates of nitrate (NO_3^-) and ammonium (NH_4^+). We found that dry-to-flow mode, irrespective of sediment transport, influenced dissolved oxygen, CO_2 fluxes, nutrient dynamics, and changes in $\delta^{15}N\text{-}N_2$, but did not affect CH_4 or N_2O fluxes. Interestingly, both dry-to-flow modes produced nearly synchronized CO_2 flux peaks upon water entry to the flumes, regardless of sediment transport rate. Yet, transport was positively associated with dissolved oxygen concentrations and net NO_3^- release and negatively related to changes in $\delta^{15}N\text{-}N_2$, CH_4, and N_2O fluxes. Our findings highlight how the mode of flow resumption and sediment transport dynamics can shape biogeochemical hot moments in rivers and underscore the need to consider the characteristics of hydrological transitions when estimating non-perennial river contributions to global carbon and nitrogen budgets.

Non-perennial rivers, which account for more than half of the global fluvial network (Messager et al. 2021), are characterized by periodic drying and flow (Datry et al. 2017). When water returns to previously dried streambeds—either as surface flow or simply through rewetting—it can trigger a pulse of microbial metabolic activity (Ryo et al. 2019) from the activation of dormant microorganisms upon the presence of water and the leaching of nutrients and carbon (Larned et al. 2010; Romaní et al. 2017; von Schiller et al. 2017). Stream microbes reactivation can lead to a sharp increase in aerobic and anaerobic processes (Arce et al. 2015; von Schiller et al. 2019; Gómez-Gener, Siebers, et al. 2021), with sediment respiration showing a mean 66-fold increase compared to dry conditions (von Schiller et al. 2019). Such an increase in metabolic activity, often referred to as a hot moment (McClain et al. 2003) or an ecosystem control point (Bernhardt et al. 2017), can occur within hours to days after flow resumption (Schreckinger

*Correspondence: clara.mendozalera@rptu.de

Associate editor: Ryan A. Sponseller

et al. 2022). However, despite the potentially important contribution of non-perennial rivers to global greenhouse gas budgets (Lauerwald et al. 2023; López-Rojo et al. 2024), the drivers that modulate these biogeochemical hot moments are not well known (Romaní et al. 2017).

The way in which surface water flow resumes can modulate biogeochemical processes (Romaní et al. 2017), and therefore, may also play a key role in controlling biogeochemical hot moments. Here, we define flow resumption as the complete re-establishment of surface flow, including complete water saturation of sediment pore space, and argue that it is characterized by two main interrelated properties: (i) *dry-to-flow mode*, that is the process by which flow is re-established, such as instant flow (e.g., flash flood) or gradual inundation by rising groundwater before surface water flow establishes, and (ii) *flow characteristics* of the re-stablished flow, such as flow velocity and turbulence, which, together with streambed properties, such as sediment grain size, may lead to sediment transport (Baas 2002; Deal et al. 2023). The mechanisms by which both dry-to-flow mode and flow characteristics modulate the hot moment can be direct or indirect. Direct effects relate to physical stress on microbial biofilms caused by the surface flow and associated sediment transport (Mackenthun and Stefan 1998; Baas 2002). Indirect effects are linked to oxygen and solute availability within sediments (Higashino and Stefan 2008), which are influenced by hyporheic exchange, the mixing of surface and subsurface waters (Boano et al. 2014), and can be modulated by sediment transport (Ahmerkamp et al. 2015). However, the combined effects of dry-to-flow mode and sediment transport on biogeochemical processes and hot moments during flow resumption, to our knowledge, have not yet been studied.

Regulation of oxygen supply during flow resumption governs biogeochemical processes and its transitions are strongly associated with dry-to-flow mode and flow characteristics. For instance, when flow gradually returns through rising groundwater, it may already carry anoxic water. Alternatively, if oxic conditions are initially present, they can quickly shift to anoxia due to increased microbial activity driven by water availability (von Schiller et al. 2019). Upon anoxic conditions, anaerobic pathways such as denitrification and methanogenesis may be promoted, resulting in hot moments of N_2, N_2O, and CH_4 fluxes (Baker et al. 1999; Groffman et al. 2009), while constraining aerobic processes like CO_2 production from aerobic respiration and nitrification (Triska et al. 1990; Gómez-Gener, Siebers, et al. 2021). Flow characteristics can change drastically during flow resumption, leading to rapid shifts in oxygen availability (Higashino et al. 2009) and consequently in biogeochemical processes. However, the extent to which sediment transport affects this biogeochemical process remains unclear. For instance, Oprei et al. (2023, 2024) observed stronger effects of light intensity and prior drying than of sediment transport, whereas other studies reported sediment transport as a major controlling factor (Zlatanovic et al., Zlatanović et al. 2017; Scheidweiler et al. 2021; Schulz et al. 2023). Therefore, the interplay between dry-to-flow mode and flow characteristics can generate complex patterns of biogeochemical hot moments, mediated by shifts in electron acceptor, nutrient availability, and physical stress.

Here we tested whether the mode of dry-to-flow and flow characteristics influence carbon (C) and nitrogen (N) biogeochemical hot moments over 24 h upon flow resumption. Using a flume setup, we examined two distinct dry-to-flow modes: instant and gradual, the latter with a 6-h inundation stage simulating groundwater rise prior to flow resumption. After the surface water flow was established (within seconds for instant, and after 6 h for gradual), flumes were set to one of six different flow velocities (from 0.13 to 0.21 m s^{-1}) which resulted in increasing sediment transport (0 to 11.88 g m^{-1} s^{-1}). We hypothesize that in the gradual mode, anoxic conditions will establish prior to flow resumption—especially in deeper sediment layers—leading to higher CH_4 and N_2O fluxes and $\delta^{15}N\text{-}N_2$ (as a proxy for denitrification following the addition of a $^{15}N\text{-}NO_3^-$ tracer to the water column), and lower CO_2 fluxes and nitrification. Consequently, NO_3^- release from sediments layer to the overlying water and NH_4^+ uptake via nitrification are both expected to decrease compared to the instant mode at the same sediment transport rates. Secondly, we hypothesize that as flow velocity and associated sediment transport increase, oxic conditions within the deeper sediment porewater will increase, promoting CO_2 fluxes and nitrification while reducing CH_4, N_2O fluxes, and $\delta^{15}N\text{-}N_2$.

Materials and methods

Sediment collection

In May 2023, sediment samples were collected from the river Queich (49.2269°N, 8.3821°E) near Germersheim, Germany, from a sandy reach characterized by migrating ripples and dunes. Surface sediment (5 cm depth) was collected within a 100-m river reach. On site, sediments were sieved through a 2-mm mesh to remove larger elements such as gravel, wood pieces, and macroinvertebrates, homogenized, and then distributed into 17 Polypropylene boxes (60 × 40 × 12 cm), each containing 12 L of sediment. The sediment-filled boxes were transported to the lab (40-min drive), where the sediment was dried for 38 d in darkness at a constant temperature (20°C) to maintain homogeneous conditions until volumetric water content, measured weekly in mid-sections of five boxes, reached a low stable value of 1.30% ± 0.07% (Fig. 1a). Volumetric water content was measured using an SMT100 soil moisture sensor (Truebner GmbH), and the boxes were tilted throughout the drying phase to facilitate water drainage through ⌀ 0.5-cm drainage holes. The collected sediment had an organic matter content

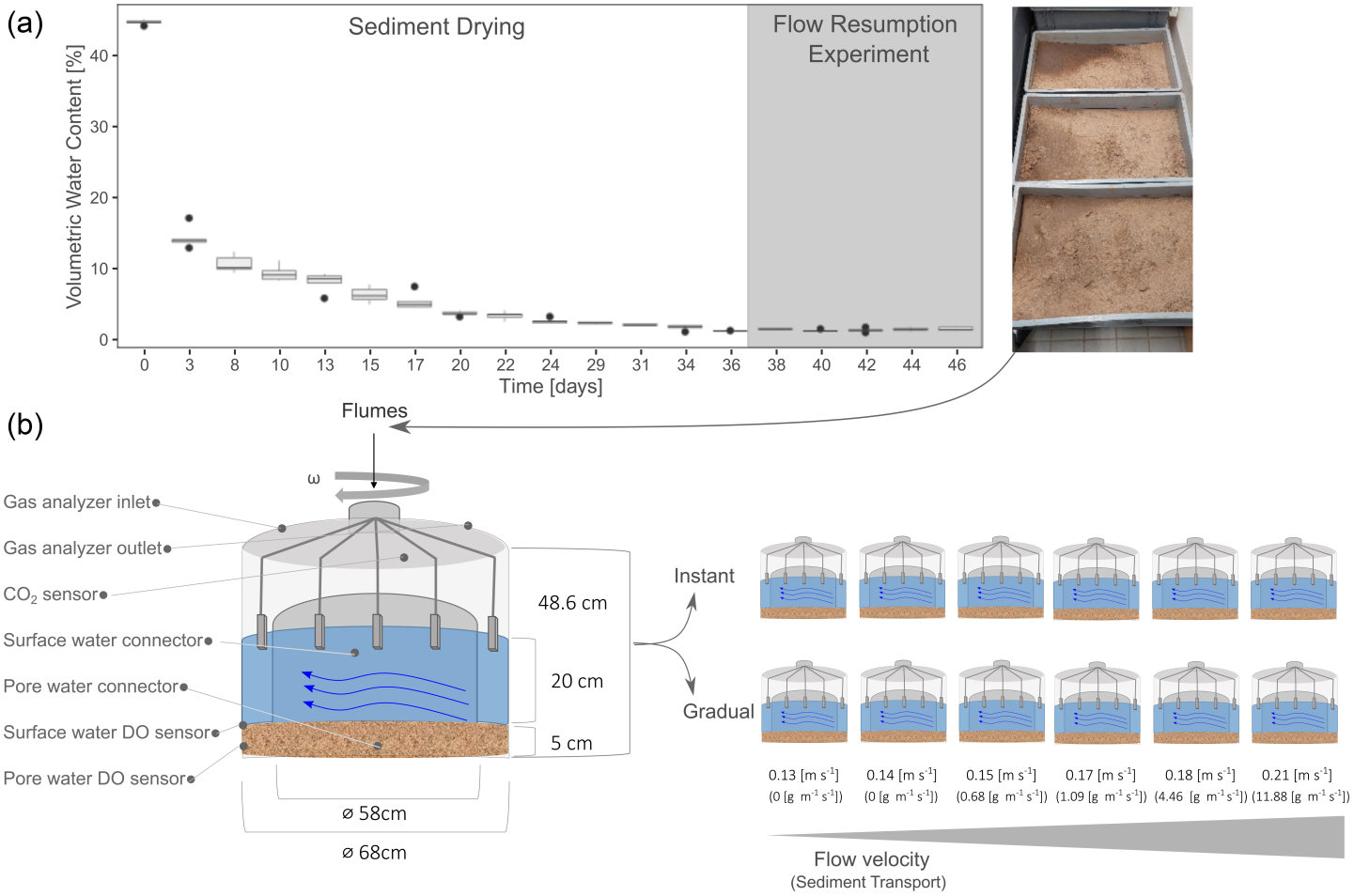

Fig. 1. (**a**) Changes in sediment volumetric water content over the 38-d drying period. (**b**) Schematic representation of flume setup and experimental design.

of 4.38 ± 0.9 mg ash-free dry weight (AFDW) g^{-1} dry weight (DW) and a 50th percentile particle diameter (D_{50}) of 438.29 ± 8.70 μm. Organic matter was determined by loss on ignition (3 h at 550°C), and particle size distribution was assessed by dry sieving, using a mechanical shaker, of ignited sediment through meshes of 1, 0.5, 0.25, and 0.063 mm.

Experimental setup

Six gas-tight acrylic glass cylindrical flumes (48.4 cm high with a 68 cm diameter) containing a smaller closed plexiglass cylinder (38.4 cm high with a 58 cm diameter) centered and fixed at the bottom, creating a circular space of 10 cm width between the inner and larger cylinder that conforms the actual flume experimental area (Fig. 1b). The lid (82 cm diameter) had a motor with eight paddles fitting the flume area, allowing rotation for flow generation. The lid was equipped with an inlet and outlet connected in a closed loop to a CO_2 and CH_4 gas analyzer (Los Gatos Research, Inc.) and the loop tubing included a septum for gas sampling. On the inner part of the lid, a CO_2 sensor (K33 LP T, Senseair AB) was attached for continuous measurement of CO_2 mixing ratios in the flume headspace. Additionally, fiber optic oxygen sensors (FireSting O_2, PyroScience GmbH, Germany) were installed in the flume wall at heights of 2 and 5 cm (Fig. 1b). Sediment pore and surface water were sampled through connectors placed in each flume wall at heights of 2 and 15 cm, respectively (Fig. 1b).

The experimental design consisted of two dry-to-flow modes (instant and gradual) and six flow velocities (0.13, 0.14, 0.15, 0.17, 0.18, and 0.21 m s^{-1}) covering a range of sediment transport ranging from no transport to migrating dunes (*see* below). Each treatment was replicated three times, resulting in a total of 36 replicates (2 dry-to-flow modes × 6 flow velocities × 3 replicates) (Fig. 1b). We replicated the experiment in time, which resulted in six runs, three runs for gradual mode and three for instant mode. In each run, each flume corresponded to one velocity level.

Once the sediment was dry, each flume was filled with 7.5 kg of dry sediment (5 cm sediment depth) and 23.5 L of artificial stream water (20 cm water column), leaving a 20.71 L headspace. Artificial water was prepared using tap water

enriched in dissolved organic carbon (6.97 mg L^{-1}), NO_3^- (9.57 mg L^{-1}), NH_4^+ (1.27 mg L^{-1}) and PO_4^{3-} (0.87 mg L^{-1}) to mimic river Queich conditions (Sampling site point: 2377526000 Rheinland Pfalz Landesamt für Umwelt). Dissolved organic carbon was enriched using a leachate prepared from Alder leaves collected in 2021 in the Palatinate forest and air-dried. The obtained leachate had approximately 164 mg dissolved organic carbon per liter achieved by soaking 10 g of dry leaves in 1 L of water for 24 h with a pressure air stone, followed by sieving the leachate through a 63-μm mesh. Dissolved organic carbon leachate was analyzed with an aqueous elemental analyzer (multiNC 2011S, Analytik Jena). Before each run, the water for each flume was acclimated for 1 d at 20°C in an open container. For the instant treatment, after the sediment was placed in the flumes, water was gently added (23.5 L) at once to each flume, avoiding any sediment resuspension, then the lid was placed and gas-tight sealed, the headspace was flushed with compressed air to establish constant initial CO_2 and CH_4 concentrations across experiment runs, and the flow started and ran for 24 h. To quantify denitrification as $\delta^{15}N\text{-}N_2$ (*see* below), the water column was spiked upon flow resumption, also for gradual treatment, with $^{15}N\text{-}NO_3^-$ (1.4 mg L^{-1}). The tracer is included in the background NO_3^- concentration (9.57 mg L^{-1}) and was added via the water-sampling connector at 15 cm above the sediment in the water column (Fig. 1b). For the gradual dry-to-flow mode, a peristaltic pump connected to the flume wall (1 cm above the bottom of the flume) slowly saturated the sediment of each flume at a rate of 163 mL min^{-1} over 6 h until 23.5 L of artificial water was added and a water column of 20 cm was created. Then, the lid was placed at the end of the 6 h of inundation stage, the headspace was flushed with compressed air and flow started as for instant dry-to-flow mode.

Flow velocity and sediment transport rate determination

To quantify flow velocity and sediment transport rates, an additional flume was adapted to accommodate an electromagnetic flow meter (OTT MF Pro flowmeter, OTT HydroMet GmbH). The flume was filled as described above and the probe was placed 1 cm above the sediment surface, and 12 measurements were recorded every 5 s for a minute after allowing 10 min for stabilization at each flow velocity level.

Sediment transport rate was determined based on the displacement of bedforms (mainly ripples and dunes, hereafter referred to as dunes). Time-lapse videos were recorded using a GoPro Hero 9 camera, capturing images at a 5-s interval, Full HD resolution (RGB 1920 × 1080), and narrow lens mode. Marks, placed at 5-cm intervals along the inner wall of the flumes, were used to monitor the displacement of each dune crest. MATLAB R2022b's Video Viewer tool was employed to correct distortion and process time-lapse videos. From the number of frames needed for a crest to move 10 cm, dune celerity (Uc, cm h^{-1}) was determined. Additionally, time-lapse videos with a vertical metric reference (with 0 cm at the sediment bottom) fixed to the outer flume wall were used to determine dune height (H, m). Images were captured every 5 s and compiled into time-lapse videos exported at 30 frames s^{-1}, such that a 150-s video represented 6.25 h of real time. Sediment height was measured at the same reference point every second on time-lapse videos (equivalent to 2.5-min intervals in real time) and the maximum dune height was estimated from the resulting profile over an approximately 60-min period (Supporting Information Fig. S1). Following Van den Berg (1987), the sediment transport rate (Sc, g m^{-1} s^{-1}) was determined as follows:

$$\mathrm{Sc} = \frac{1}{2}\rho s(1-\varepsilon)UcH \quad (1)$$

where ρs (g L^{-1}) is sediment density and ε corresponds to porosity. This formula assumes dunes to be triangular in a cross-section and we additionally assume a ρs sand of 1600 g L^{-1} and ε of 0.2 (Mendoza-Lera et al. 2017). The relationship between sediment transport rate and flow velocity followed an exponential function (Supporting Information Fig. S2) with an R^2 of 0.94. No sediment transport was observed at the two lowest velocities, 0.13 and 0.14 m s^{-1}.

CH_4 and CO_2 fluxes

A Los Gatos Research Gas Analyzer was connected in a closed loop to the inlet and outlet ports on the flume's lid to measure changes in CH_4 and CO_2 mixing ratios (in ppmv) in the headspace. Measurements were taken 30 min after flushing the flumes with compressed air (0 h). Flushing was performed only at the start of each run, and subsequently measurements at 12 and 24 h from the start of each run were also taken. Each measurement was conducted over 20 min in a closed loop. To continuously measure CO_2 production, K33 LP T CO_2 sensors placed inside the lid of each flume continuously recorded CO_2 concentrations at 1-min intervals. The CH_4 and CO_2 mixing ratios (ppmv) were converted to fluxes (mmol CO_2 m^{-2} d^{-1} and CH_4 μmol m^{-2} d^{-1}) for 0–12, 12–24, and 0–24 h periods using slopes from linear fits of concentration change during each measurement. Similarly, CO_2 mixing ratios (ppmv) from the K33 LP T sensor measuring CO_2 continuously in each flume were converted to fluxes (mmol CO_2 m^{-2} d^{-1}) on an hourly basis using slopes of linear fits, after correcting each sensor's values against a Los Gatos Research Gas Analyzer measurement. Atmospheric pressure and temperature, used to convert mixing ratios to fluxes, were obtained from a room data logger TFA LOG210 PDF Thermo-Hygro (TFA Dostmann GmbH & Co. KG) placed in the same room. The flux estimates considered the flumes' headspace volume (0.021 m^3) and are expressed per flume area (0.099 m^2). Additionally, the mixing ratios of CH_4 and CO_2 from dry sediment were measured prior to each run using a closed 5 L chamber with a 5 cm sediment layer, as in the flumes, connected to a

gas analyzer for 20 min. Approximately 1.5 kg of sediment was used, covering an area of 0.02 m^2.

Change in $\delta^{15}N\text{-}N_2$ and N_2O fluxes

At the start (0 h) and end (24 h) of each run, 2 mL of headspace gas was collected for $\delta^{15}N\text{-}N_2$ isotope gas and 12 mL of headspace gas for N_2O concentration determination. Using 5 mL syringes for $\delta^{15}N\text{-}N_2$ and 20 mL syringes for N_2O, headspace air samples were collected through the septum on the tubing connecting the flumes with the Los Gatos Research Gas Analyzer (closed loop) while the gas analyzer was on, ensuring complete mixing of the headspace, and transferred into helium-flushed and pre-evacuated 12-mL Exetainer vials (Labco Ltd., Ceredigion, UK). N_2 isotopic composition was determined at the SOWA Research Infrastructure (Biology Centre, Czech Academy of Science) using a GasBench II peripheral interfaced with a MAT253 Plus isotope ratio mass spectrometer via a ConFlo IV device (Thermo Scientific). Briefly, a double-holed needle was used to purge the headspace sample in the Exetainer through a Nafion water trap and into a 250 μL sample loop, which was then injected onto a Carboxen PLOT 1010 (0.53 mm ID; Supelco) held at 70°C with a flow rate of 2.2 mL min^{-1}, to separate N_2 from other gases. The δ-values of N_2 (‰) were determined for two replicated injections, relative to a working N_2 gas cylinder, and corrected for linearity and finally normalized to the $\delta^{15}N_2$-Air scale. The external precision for injections of air N_2 was $\pm$ 0.3‰. N_2O mixing ratios were determined through gas chromatography (SRI8610, SRI) with an electron capture detector and N_2 as carrier gas. Calibration was achieved with a certified calibration standard containing 0.88 ppmv N_2O. N_2O concentrations were calculated from measured headspace mixing ratios (ppmv) using temperature-dependent Henry's law constants (Sander 2015), and subsequently converted to fluxes (mmol N_2O m^{-2} d^{-1}) based on the difference between the initial (0 h) and final (24 h) mixing ratio values and expressed per flume area (0.099 m^2).

Porewater CO_2, CH_4, and N_2O concentrations

At the end of each treatment (24 h after the start of flow), 10 mL of pore water was extracted from a height of 2 cm above the flume bottom using a 50-mL syringe. A 20 mL headspace volume was created in the syringe with pure N_2 gas (Stickstoff Premium-Air Products). The water sample and headspace were equilibrated by shaking, after which 13 mL of the headspace was transferred into a 12 mL pre-evacuated Exetainer vial. CO_2, CH_4, and N_2O concentrations were determined using a gas chromatograph (SRI8610, SRI) equipped with a flame ionization detector with methanizer and an electron capture detector, using N_2 as the carrier gas. Calibration was performed with a certified calibration standard. Dissolved concentrations of CO_2, CH_4, and N_2O were calculated based on the measured mixing ratios using temperature-dependent Henry's law coefficients (Sander 2015) and expressed per flume area (0.099 m^2).

Net nutrient release and uptake rates

Water samples for nitrate (NO_3^-), ammonium (NH_4^+), and orthophosphate (PO_4^{3-}) analysis were collected from the water column both before and at the end of each treatment run. The samples were filtered through 0.45-μm filters (Micropur PA, Altmann Analytik) and stored at −20°C for approximately 2 months before shipment for analysis. NO_3^- and NH_4^+ concentrations were measured using a continuous flow analyzer (AutoAnalyzer 3, SEAL Analytical; Bran + Luebbe) according to ISO standards 13395/DIN 38 405, 14256-2, and 14255. PO_4 concentration was determined photometrically using the molybdenum blue method (Murphy and Riley 1962) with a Continuous Flow Analyzer (CFA Autoanalyzer, Bran + Luebbe). Nutrient net uptake and release rates were estimated by calculating the difference between initial and final concentrations for 24 h and expressed per flume area (0.099 m^2).

Data analysis

All statistical analyses were conducted in R (R Core Team, 2022, version 4.2.2) with a significance threshold of $\alpha = 0.05$. Generalized additive mixed models (GAMMs) were applied using the gam function from the "mgcv" package (Wood 2017). Response variables included dissolved oxygen (shallow and deeper layers), gas fluxes (CH_4, CO_2, N_2O), changes in $\delta^{15}N\text{-}N_2$, porewater gas concentration (CH_4, CO_2, N_2O) and net nutrient uptake/release rates (NH_4^+, NO_3^-, PO_4^{3-}). Models incorporated smooth terms for sediment transport with $k = 5$ basis functions, included dry-to-flow mode (instant or gradual) as a main effect, modeled the interaction between sediment transport and dry-to-flow mode using a smooth term with $k = 5$, and treated replicate runs as a random factor. For CH_4 and CO_2 fluxes, models were run over three periods: 0–12, 12–24, and 0–24 h to capture shorter-term dynamics. Single models for N_2O flux, change in $\delta^{15}N\text{-}N_2$, and sediment net nutrient release/retention rates (NO_3^-, NH_4^+, and PO_4^{3-}) were generated for the 0–24 h experimental period. Models for porewater CO_2, CH_4, and N_2O concentrations were focused only on the final concentration in treatments. For dissolved oxygen, models were applied to each sediment depth layer (shallow and deep), with $k = 4$ for the interaction between sediment transport and dry-to-flow mode. For each response variable, we compared a full model including sediment transport, dry-to-flow mode, their interaction, and run as a random effect with reduced models excluding each one of the previously mentioned components. Model support was evaluated using likelihood-ratio tests and Akaike's Information Criterion (AIC), allowing assessment of the relative importance of sediment transport, dry-to-flow mode, and their interaction in explaining variation in each response. Finally, to track the

temporal dynamics of CO_2 flux, hourly estimates of CO_2 flux were plotted over time using package "ggplot2."

Results

Dissolved oxygen

Overall, the average dissolved oxygen concentrations in the shallow sediment layer ranged from 59.7% to 92.80% for the instant mode and from 7.6% to 84.2% for the gradual mode. In deeper sediments, concentrations ranged from 10.2% to 84.7% (instant) and 0% to 70.3% (gradual) (Fig. 2). At the shallow sediment layer, dissolved oxygen under instant mode significantly increased linearly with sediment transport, showing a 1.5-fold increase from no transport to the maximum rate applied in our experiment (12 g m^{-1} s^{-1}) (Supporting Information Table S1; Fig. 2). In contrast, in the gradual mode, the shallow layer showed a significant non-linear increase in oxygen concentrations (Supporting Information Table S1; Fig. 2). In the deeper layers, both flow modes exhibited a non-linear, significant rise in oxygen concentrations with sediment transport, stabilizing at around 6 g m^{-1} s^{-1}. Despite similar patterns, oxygen levels under instant mode were on average 1.7 times higher than those under the gradual mode. Dissolved oxygen responses among models differed between depths (Supporting Information Table S2). In the deeper sediment layer, the best model excluded the interaction term while at the shallow layer, the full model was retained (Supporting Information Table S2).

During the inundation stage in the gradual mode, dissolved oxygen in the deeper sediments dropped to anoxic levels (below 5% dissolved oxygen) after 2.9 h of rewetting and after 3.2 h in the shallow sediment layer. Upon flow resumption, shallow sediments in the gradual mode rapidly returned to oxic conditions, and shallow sediments in both the instant and gradual modes remained oxic throughout the experiment (Supporting Information Figs. S3, S4). In contrast, in the deeper sediments, oxygen dynamics depended on sediment transport in both dry-to-flow modes, remaining anoxic in the absence of transport but shifting, at least temporarily, to oxic conditions when transport occurred (Supporting Information Figs. S3, S4). Sediment transport also regulated the 24 h dissolved oxygen dynamics in shallow and deep layers measured every minute (Supporting Information Fig. S4). Changes in dissolved oxygen were smoother in shallow layers across all sediment transport rates for both instant and gradual treatments. Remarkably, in the deep layer, both modes showed continuous and drastic changes in dissolved oxygen dynamics between sediment transport rates of 4.5 and 11.9 g m^{-1} h^{-1} (Supporting Information Fig. S4).

CO_2 fluxes

CO_2 fluxes ranged from 10 to 80 mmol m^{-2} d^{-1} following flow resumption, while during the dry phase, mean fluxes were 11.0 ± 5.8 mmol m^{-2} d^{-1}. Over the full 24-h period,

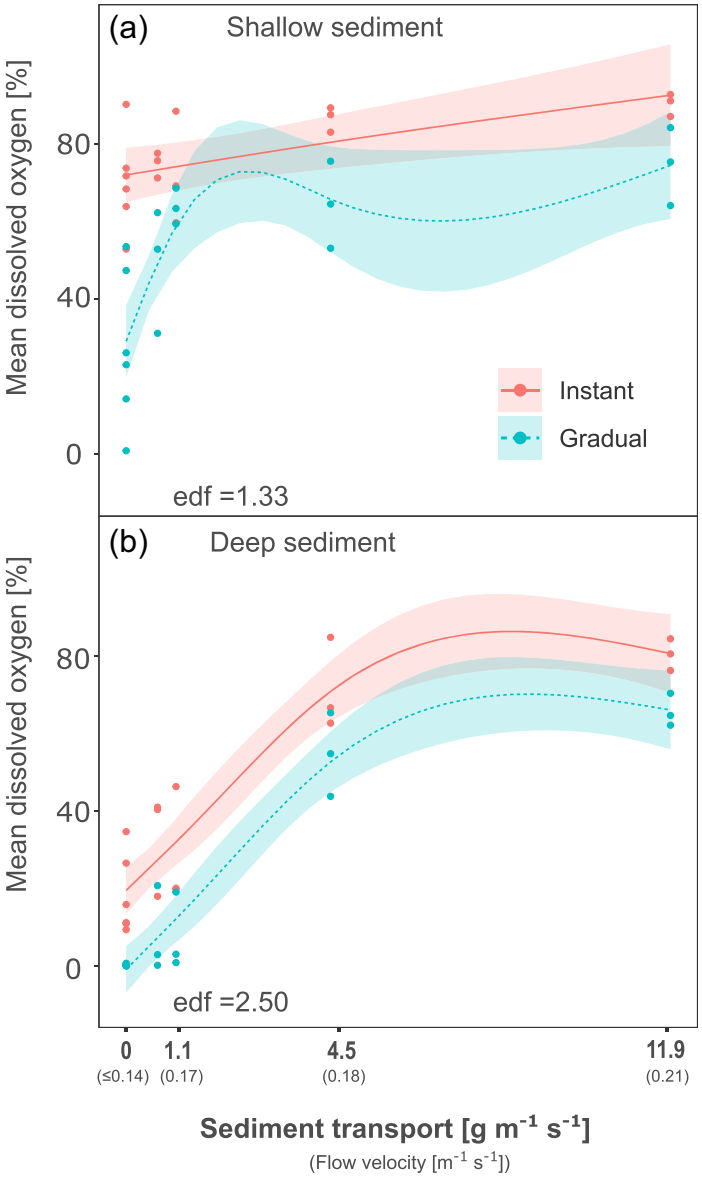

Fig. 2. (**a**) Shallow sediment layer and (**b**) deep sediment layer mean dissolved oxygen across the sediment transport gradient over 24 h following flow resumption for instant and gradual dry-to-flow modes (the 6-h inundation period preceding the gradual mode is not included). Lines show generalized additive mixed model (GAMM)–predicted smooth relationships between sediment transport rate and each variable, with the respective confidence interval as shaded areas.

CO_2 fluxes were not significantly influenced by either sediment transport or dry-to-flow mode (Fig. 3; Supporting Information Table S1). However, when split into two 12-h periods, different patterns emerged. During the first 12 h, gradual mode produced significantly higher fluxes, approximately three times those of the instant mode, across all sediment transport rates (Fig. 3; Supporting Information Table S1). In contrast, between 12 and 24 h, this trend reversed, with instant mode showing fluxes approximately twice as high as

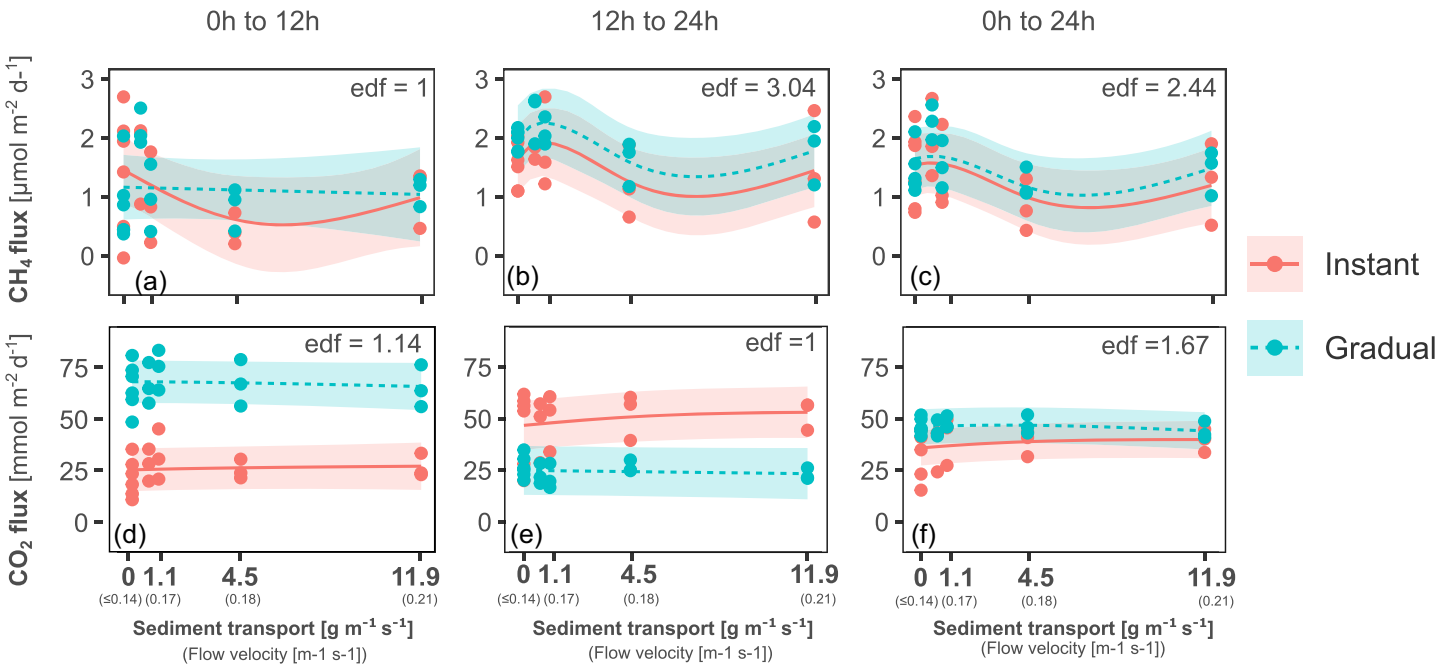

Fig. 3. CO_2 and CH_4 fluxes as a function of sediment transport rate over 24 h following flow resumption for instant and gradual dry-to-flow modes (the 6-h inundation interval for the gradual mode is not included). (**a**–**c**) CH_4 fluxes and (**d**–**f**) CO_2 fluxes for the following time periods for 0–12 h (**a**, **d**), 12–24 h (**b**, **e**), and 0–24 h (**c**, **f**). Lines represent generalized additive mixed model (GAMM)–predicted smooth relationships between sediment transport rate and gas fluxes, with shaded areas indicating confidence intervals.

the gradual one. Model comparisons showed period-dependent dynamics (Supporting Information Table S2), where during the first 12 h, the best model excluded sediment transport. In contrast, over the full 24 h and during the 12- to 24-h periods, the full model was the best supported.

CO_2 fluxes temporal dynamics

Hourly CO_2 flux estimates revealed distinct timing of peak fluxes within the first 24 h of flow resumption, occurring in both dry-to-flow modes and independent of sediment transport (Fig. 4). In the instant mode, the maximum CO_2 flux (91.3 ± 7.4 mmol m^{-2} d^{-1}) occurred 15.5 ± 2.6 h after flow resumed. In contrast, the gradual mode peaked earlier, with a maximum flux of 95.9 ± 12.6 mmol m^{-2} d^{-1} occurring at 7.0 ± 1.6 h, which corresponds to 13.0 ± 1.6 h after water saturation started in the sediment (6 h before flow initiation; Fig. 4). On average, maximum CO_2 fluxes under both instant and gradual treatments were 8.3 and 8.7 times higher, respectively, than the CO_2 flux measured in dry sediment (11.0 ± 5.7 mmol m^{-2} d^{-1}).

CH_4 fluxes

Overall, CH_4 fluxes ranged from 0 to 3 μmol m^{-2} d^{-1} with high variability among replicates (Fig. 3), while CH_4 uptake was observed during the dry phase (-1.0 ± 1.8 μmol m^{-2} d^{-1}). Over the 24-h flow resumption, the dry-to-flow mode did not affect CH_4 fluxes. However, they showed a time-dependent effect of sediment transport. In the first 12 h, sediment transport was slightly, and not significantly, correlated with the CH_4 fluxes. However, after 12 h, the influence of sediment transport became stronger and significant with a nonlinear decreasing trend (Fig. 3; Supporting Information Table S1). Although sediment transport deviance explained was higher over the full 24-h than during the first 12-h, it explained less than in the 12- to 24-h period, and the 24-h relationship was nonsignificant (Supporting Information Table S1). Generalized additive mixed model comparisons revealed temporal differences in the drivers of CH_4 flux (Supporting Information Table S2). During the first 12 h, the best-supported model excluded sediment transport while across the full 24 h and particularly during the 12–24 h period, models excluding dry-to-flow mode were favored (Supporting Information Table S2).

N_2O flux

N_2O fluxes ranged from 0 to 40 μmol m^{-2} d^{-1}. Although not statistically significant, fluxes tended to be higher under the gradual dry-to-flow mode compared to the instant mode (Fig. 5; Supporting Information Table S1). Regardless of dry-to-flow mode, N_2O fluxes peaked in the absence of sediment transport and progressively decreased, stabilizing around a sediment transport rate of 2.5 g m^{-1} s^{-1}. The best-supported model over 24 h period excluded dry-to-flow mode (Supporting Information Table S2).

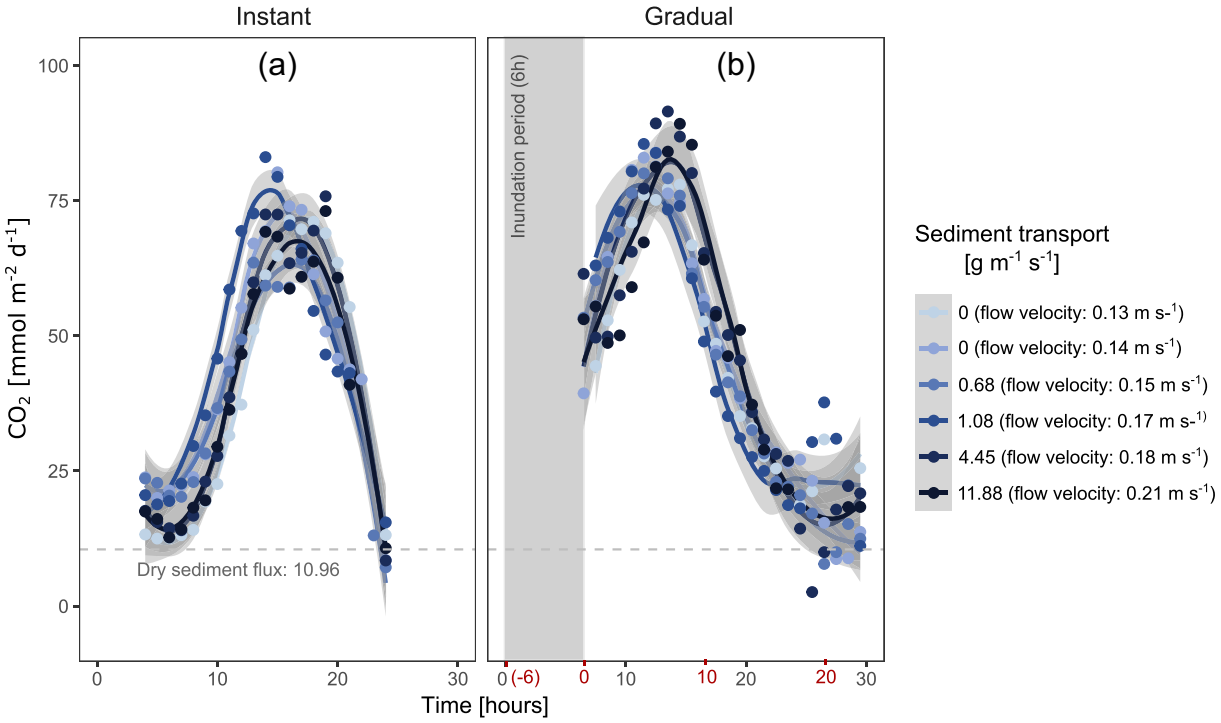

Fig. 4. Smooth conditional means of hourly CO_2 flux rates measured using K33 Sensair sensors among (**a**) Instant and (**b**) Gradual treatments, across different sediment transport velocities. The shaded gray area marks the inundation period, and the red *x*-axis labels indicate time since the start of flow resumption surface flow.

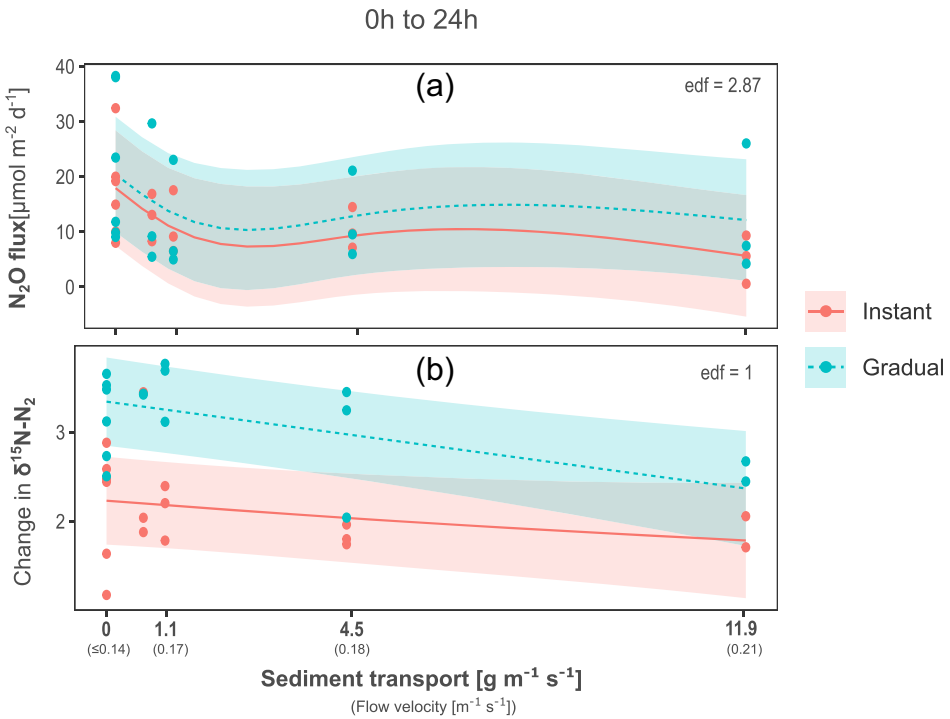

Fig. 5. (**a**) N_2O fluxes and (**b**) changes in $\delta^{15}N$-N_2 with sediment transport rate over the 0- to 24-h period following flow resumption for instant and gradual dry-to-flow modes (the 6-h inundation interval preceding the gradual mode is not included). Lines show generalized additive mixed model (GAMM)–predicted smooth relationships between sediment transport rate and each variable with the respective confidence interval as shaded areas.

Change of $\delta^{15}N\text{-}N_2$

The change in $\delta^{15}N\text{-}N_2$, derived from the $^{15}N\text{-}NO_3^-$ spike added at flow start, is a measure of the proportion of ^{15}N relative to ^{14}N, which ranged from 1 to 4. Over the 24-h flow resumption period, the gradual mode exhibited higher initial $\delta^{15}N\text{-}N_2$ values and a steeper linear decline with increasing sediment transport rates compared to the instant mode, which showed a less pronounced decline (Fig. 5; Supporting Information Table S1). At the highest sediment transport rates, both modes converged, displaying similar changes in $\delta^{15}N\text{-}N_2$ values. Changes in $\delta^{15}N\text{–}N_2$ were best described by GAMM model excluding dry-to-flow mode over 24 h period (Supporting Information Table S2).

Porewater CO_2, CH_4, and N_2O gas concentrations

Porewater concentrations ranged from 61.9 to 177 μmol L^{-1} for CO_2, 0 to 1.4 μmol L^{-1} for N_2O and 0 to 0.10 μmol L^{-1} for CH_4 (Supporting Information Table S1; Supporting Information Fig. S5). Neither dry-to-flow mode nor sediment transport significantly influenced the concentrations of CH_4, CO_2, or N_2O in porewater. However, the lower-range concentrations of all three gases were considerably higher than their equilibrium concentrations in water under the experimental conditions, calculated at 13.9 μmol L^{-1} for CO_2, 0.008 μmol L^{-1} for N_2O and 0.002 μmol L^{-1} for CH_4. For porewater CH_4 and N_2O, the best-supported models excluded dry-to-flow mode. For porewater CO_2, the best model excluded sediment transport.

Net nutrient release and uptake rates

We observed net release of NO_3^- and net NH_4^+ and PO_4^{3-} uptake by the sediment. Net NO_3^- release ranged from 0 to 4 μg NO_3^- m^{-2} h^{-1}. Over the 24-h period, net NO_3^- release was significantly higher under the gradual mode, despite both flow modes showing similar patterns across sediment transport rates (Supporting Information Fig. S6; Supporting Information Table S1). Sediment transport had a significant nonlinear effect, with net NO_3^- release increasing as sediment transport increased. Generalized additive mixed model comparisons for net NO_3^- release were best described by models excluding dry-to-flow mode (Supporting Information Table S2).

Net NH_4^+ uptake rates ranged from 0.4 to 0.6 μg NH_4^+ m^{-2} h^{-1}. After 24 h, most net NH_4^+ concentrations dropped below detection limits, suggesting near-complete uptake. Given that concentrations fell below detection limits, the reported uptake rates represent minimum possible net uptake rates, and caution should be exercised when interpreting the results (Supporting Information Fig. S6; Supporting Information Table S1). Net uptake rates were similar across treatments, except for the lowest sediment transport rate under the gradual mode, which had the lowest uptake (Supporting Information Fig. S6; Supporting Information Table S1). No significant relationship was found between net NH_4^+ uptake and sediment transport. Generalized additive mixed model comparisons for net NH_4^+ uptake were best explained by the full model, suggesting combined influences of sediment transport and dry-to-flow mode (Supporting Information Table S2).

Net PO_4^{3-} uptake ranged from 0.10 to 0.40 μg net PO_4^{3-} m^{-2} h^{-1}. Over the 24-h period, both instant and gradual treatments exhibited similar linear trends in net PO_4^{3-} uptake with increasing sediment transport. However, net uptake rates were consistently lower under the gradual mode than in the instant one (Supporting Information Fig. S6; Supporting Information Table S1). Net PO_4^{3-} dynamics were best explained by the full GAMM (Supporting Information Table S2).

Discussion

We tested how the mode of dry-to-flow transition and sediment transport jointly regulate biogeochemical hot moments upon flow resumption. We hypothesized that a gradual dry-to-flow transition would promote anoxic conditions prior to flow return, thereby enhancing CH_4 production, N_2O emissions, and complete denitrification while suppressing CO_2 fluxes and nitrification. We further expected that increasing sediment transport would reverse these patterns by enhancing sediment oxygenation. Overall, we found that the mode of flow resumption and sediment transport jointly regulated dissolved oxygen dynamics, especially in deeper sediments. While dry-to-flow mode and particularly sediment transport were more relevant for C and N anaerobic processes, the mere presence of water, regardless of flow mode, was the primary driver of CO_2 emission hot moments.

Dissolved oxygen dynamics

As predicted by our first and second hypotheses, the gradual dry-to-flow mode reduced dissolved oxygen concentrations, whereas increasing sediment transport rates enhanced deep sediment dissolved oxygen levels in a non-linear way. The mechanisms by which sediment transport increased oxygen are likely to reflect a combination of enhanced flow and particle movement (Higashino et al. 2009; Ahmerkamp et al. 2015). Twenty-four–hour average dissolved oxygen concentration showed a plateau at the highest transport rates, a pattern that may indicate reduced oxygen exchange at high sediment transport intensities, potentially caused by sediment transport altering the pressure gradients that control porewater advection (Ahmerkamp et al. 2015). The intense oscillations in oxygen concentration observed at high sediment transport rates may reflect changes in sensor position relative to the sediment surface, as dunes were larger and migrated more rapidly under these higher flow conditions. Nevertheless, these results show that dissolved oxygen variability persists even under high flow velocities. More broadly, our findings indicate that sediment transport can enhance oxygen penetration into deeper sediments, although this effect seems to weaken at high transport intensities,

highlighting the role of sediment transport in shaping oxygen availability within sediments.

Aerobic processes

We also predicted that CO_2 fluxes and nitrification will be more impacted by instant mode compared to gradual, and at intermediate sediment transport rates. Our results indicate that, once surface flow was initiated, the gradual resumption mode exhibited higher CO_2 fluxes for the first 12 h and then the relationship shifted, such that instant flow induced higher fluxes. Our CO_2 flux estimates align with nighttime estimated values reported in a global survey of streams and rivers (Gómez-Gener, Rocher-Ros, et al. 2021). However, the hourly CO_2 flux estimates peaked at almost the same time after water had entered the system ($\sim$ 14 h), regardless of the start of surface flow. Such pulse of activity can be attributed to the availability of water, which presumably reactivated dormant microorganisms, by facilitating nutrient leaching, and releasing accumulated carbon from the preceding dry phase (Larned et al. 2010; Romaní et al. 2017; von Schiller et al. 2017). These observations suggest that the presence of water is a major driver for defining the hot moment, as proposed by the Birch effect (Birch 1958). The rapid decomposition of reactive organic compounds, typically within 48 h (Hotchkiss and Del Sontro 2023), may explain the initial spike in CO_2 fluxes until approximately 14 h, after which the availability of labile organic compounds or nutrients likely became limiting. However, based on our results, this limitation does not appear to be driven by NO_3^-, NH_4^+, or PO_4^{3-} availability, and is therefore possibly linked to the depletion of labile organic matter. Early resource depletion may have overshadowed the influence of sediment transport or dry-to-flow mode, ultimately leading to a pulse-like response, similar among all treatments. Such a pattern also highlights a potential limitation of our controlled experimental settings, where substrate or nutrient exhaustion can be linked to the closed system conditions that constrain some biogeochemical processes over time, yet similar substrate or nutrient exhaustion can be expected in natural systems. Nevertheless, this highlights the importance of capturing fine-scale temporal resolution of biogeochemical processes during flow resumption.

Dry-to-flow mode and sediment transport influenced NO_3^- net release rates, but not NH_4^+ uptake during flow resumption. However, NH_4^+ concentrations fell below detection limits after 24 h in most treatments, indicating near-complete consumption. All treatments exhibited net NH_4^+ uptake and NO_3^- release, suggesting nitrification as the dominant process, consistent with previous in situ field measurements (Skoulikidis and Amaxidis 2009) and with literature synthesis of drying–rewetting processes (Skoulikidis et al. 2017). Gradual treatments with lower sediment transport showed the lowest NH_4^+ uptake, where nitrification was limited by lower dissolved oxygen levels (Strauss and Lamberti 2000). In contrast, net NO_3^- release increased with sediment transport, likely reflecting enhanced nitrification and inhibition of denitrification under higher oxygen availability (Strauss and Lamberti 2000; Groffman et al. 2009). The higher NO_3^- concentrations observed in gradual treatments may result from ammonification via mineralization of organic matter during the 6-h inundation preconditioning, with rapid NH_4^+ conversion to NO_3^- via nitrification (Rysgaard et al. 1996).

Anaerobic processes

Sediment transport significantly affected CH_4 and N_2O fluxes, as well as changes in $\delta^{15}N\text{-}N_2$, supporting our second hypothesis that with increasing sediment transport, CH_4, N_2O, and denitrification fluxes would be lower. The increase in surface water flow together with sediment transport increased the dissolved oxygen concentration in deeper sediment layers, thereby hindering anaerobic processes. We proposed that for the same sediment transport velocity, the gradual dry-to-flow mode would have promoted anoxic conditions in pore water over a longer time interval and thereby enhanced anaerobic-related fluxes. However, such a response was only observed for changes in $\delta^{15}N\text{-}N_2$, and not for CH_4 or N_2O fluxes. The low response of methane could be attributed to the short inundation period, which may have been insufficient for methanogenesis to fully develop (Angel, Claus, & Conrad, Angel et al. 2012) and/or to high methane oxidation (Mendoza-Lera et al. 2025). In contrast, denitrification occurs earlier in the redox chain and most denitrifiers are facultative anaerobes that can rapidly switch their metabolism once oxygen becomes depleted (Giannopoulos et al. 2017). Further, the availability of NO_3^- or other terminal electron acceptors, such as Fe^{3+} and SO_4^{2-}, may thermodynamically limit methanogenesis, even under low-oxygen conditions (Achtnich, Bak & Conrad, Achtnich et al. 1995). The delayed onset of methanogenesis and the presence of alternative electron acceptors during flow resumption likely explain why our CH_4 fluxes were two to three orders of magnitude lower than those reported in regional rivers using comparable in situ chamber approaches (Koschorreck et al. 2022) and global estimates (Rocher-Ros et al. 2023), and instead resembled those observed in dry sediments measured in situ with similar chamber methods (Paranaíba et al. 2022). Low CH_4 concentrations in the porewater further supported this interpretation, indicating that the fluxes were low not because CH_4 accumulated in the pore space and did not reach the headspace, but was in fact produced at very low rates and/or oxidized.

Although our results do not allow for the direct quantification of complete denitrification rates, shifts in $\delta^{15}N\text{-}N_2$ suggest enhanced denitrification under the gradual mode and particularly at lower sediment transport rates. In contrast, N_2O, a byproduct of incomplete denitrification, did not differ between dry-to-flow modes. Nonetheless, both N_2O fluxes and porewater concentrations were highest under no sediment transport, indicating that N_2O accumulated in the pore space but still diffused into the headspace. Incomplete denitrification

is often observed at aerobic–anaerobic interfaces (Wrage et al. 2001; Ji et al. 2015; Quick et al. 2019). As reported by Schulz et al. (2023), such transition zones are likely more prevalent at the low flow velocities in our experiment that led to zero-to-low sediment transport rates, promoting incomplete denitrification, resulting in increased N_2O fluxes and N_2O accumulation in porewater. In our study, N_2O fluxes upon flow resumption were within the range reported globally for rivers and ditches (Quick et al. 2019; Silverthorn et al. 2024), and exceeded those reported from regional rivers (Koschorreck, Knorr, & Teichert, 2022).

Across treatments, NO_3^- concentrations remained consistently high and were therefore unlikely to limit denitrification pathways, indicating that oxygen availability was the primary regulator of NO_3^- reduction to N_2 and N_2O. Such NO_3^- concentrations are, unfortunately, common in the region and can be even higher, as intensive land use has led to persistently elevated nitrate levels in surface and ground waters (Weber and Kubiniok 2022). Because denitrification requires labile organic carbon as an electron donor, its depletion may have constrained denitrification (Zarnetske et al. 2011), particularly in treatments without sediment transport where N_2O fluxes were highest. However, as N_2O and $\delta^{15}N\text{-}N_2$ were measured only once at 24 h, the extent of this potential limitation could not be assessed in our experiment. N_2O can also be produced as a by-product of nitrification (Lipschultz et al. 1981; Wrage et al. 2001). However, such a pathway is unlikely to explain the patterns observed here, as higher N_2O concentrations were associated with lower dissolved oxygen levels, whereas nitrification is an aerobic process (Gómez-Gener, Siebers, et al. 2021). Our results suggest that, upon flow resumption, streams can experience a hot moment of N_2 and N_2O fluxes to the atmosphere calling for the consideration of these emissions in global budgets (Lauerwald et al. 2023), particularly as a function of dry-to-flow mode and sediment transport, with the latter mainly driven by flow velocity.

Overall, our results show that biogeochemical hot moments during the first 24 h of dry-to-flow transitions are governed less by the dry-to-flow mode and more by flow characteristics, that is flow velocity and sediment transport, which physically reorganize the streambed sediments strongly shaping redox conditions under our experimental design. However, this conclusion applies to the 6 h duration of the gradual dry-to-flow mode used here. Under natural conditions, shorter, longer, or repeated gradual inundation phases may occur and could either attenuate or amplify dry-to-flow mode effects on biogeochemical dynamics. Also, worth noting for CO_2 and CH_4—where measurements were conducted across different time periods—dry-to-flow mode exerted a stronger influence during the early stages following flow resumption. At the same time, the consistently timed CO_2 pulse observed across treatments highlights water availability itself as the primary trigger of early CO_2 release, largely decoupled from subsequent hydrodynamic characteristics. Such strong water-driven response may partly obscure the effects of dry-to-flow mode and sediment transport during the initial CO_2 hot moment, but it should be recognized as a key biogeochemical control following flow resumption. This study therefore provides a mechanistic first step toward disentangling how flow resumption properties shape carbon and nitrogen dynamics in non-perennial rivers, with implications for predicting biogeochemical responses under shifting hydroclimatic regimes.

Author Contributions

José Schreckinger: writing – original draft, visualization, software, project administration, methodology, investigation, formal analysis, data curation and conceptualization. Matthias Koschorreck: writing – review and editing, resources, investigation. Lediane Marcon: writing – review and editing, methodology, investigation and conceptualization. Mario Brauns: writing – review and editing, resources. Simon Rudolph: writing – review and editing, software, methodology, investigation and conceptualization. Catalina Osorio-Pelaez: writing – review and editing, software, methodology, investigation, conceptualization. Travis Meador: writing – review and editing, resources and investigation. Clara Mendoza-Lera: writing – review and editing, supervision, resources, methodology, funding acquisition and conceptualization.

Acknowledgments

We thank Tanvir Ahmed and Melanie Brunn at RPTU for lab analyses support. Financial support was provided by the German Science Foundation through the FlowReSet project (ME 5498/2-1). Stable isotope measurements were supported by MEYS CZ Grant LM2015075 Projects of Large Infrastructure for Research, Development, and Innovations as well as the European Regional Development Fund-Project: research of key soil–water ecosystem interactions at the SoWa Research Infrastructure (No. CZ.02.1.01/0.0/0.0/16_013/0001782). We used ChatGPT-5 to correct grammar and improve the clarity of some sections of the text. Open Access funding enabled and organized by Projekt DEAL.

Conflicts of Interest

The authors declare no conflicts of interest.

Data Availability Statement

The data supporting the findings of this study are available in the PANGAEA data repository at https://doi.org/10.1594/PANGAEA.987877.

References

Achtnich, C., F. Bak, and R. Conrad. 1995. "Competition for Electron Donors among Nitrate Reducers, Ferric Iron Reducers, Sulfate Reducers, and Methanogens in Anoxic

Paddy Soil." *Biology and Fertility of Soils* 19: 65–72. https://doi.org/10.1007/BF00336349.

Ahmerkamp, S., C. Winter, F. Janssen, M. M. M. Kuypers, and M. Holtappels. 2015. "The Impact of Bedform Migration on Benthic Oxygen Fluxes." *Journal of Geophysical Research – Biogeosciences* 120: 2229–2242. https://doi.org/10.1002/2015JG003106.

Angel, R., P. Claus, and R. Conrad. 2012. "Methanogenic Archaea Are Globally Ubiquitous in Aerated Soils and Become Active under Wet Anoxic Conditions." *ISME Journal* 6: 847–862. https://doi.org/10.1038/ismej.2011.141.

Arce, M. I., M. M. Sánchez-Montoya, and R. Gómez. 2015. "Nitrogen Processing Following Experimental Sediment Rewetting in Isolated Pools in an Agricultural Stream of a Semiarid Region." *Ecological Engineering* 77: 233–241. https://doi.org/10.1016/j.ecoleng.2015.01.035.

Baas, J. H. 2002. "An Empirical Model for the Development and Equilibrium Morphology of Current Ripples in Fine Sand." *Sedimentology* 46: 123–138. https://doi.org/10.1046/j.1365-3091.1999.00206.x.

Baker, M. A., C. N. Dahm, and H. M. Valett. 1999. "Acetate Retention and Metabolism in the Hyporheic Zone of a Mountain Stream." *Limnology and Oceanography* 44: 1530–1539. https://doi.org/10.4319/lo.1999.44.6.1530.

Bernhardt, E. S., J. R. Blaszczak, C. D. Ficken, M. L. Fork, K. E. Kaiser, and E. C. Seybold. 2017. "Control Points in Ecosystems: Moving beyond the Hot Spot Hot Moment Concept." *Ecosystems* 20: 665–682. https://doi.org/10.1007/s10021-016-0103-y.

Birch, H. F. 1958. "The Effect of Soil Drying on Humus Decomposition and Nitrogen Availability." *Plant and Soil* 10: 9–31. http://www.jstor.org/stable/42931743, https://doi.org/10.1007/BF01343734.

Boano, F., J. W. Harvey, A. Marion, et al. 2014. "Hyporheic Flow and Transport Processes: Mechanisms, Models, and Biogeochemical Implications." *Reviews of Geophysics* 52: 603–679. https://doi.org/10.1002/2012RG000417.

Datry, T., N. Bonada, and A. J. Boulton. 2017. "General Introduction." In Intermittent Rivers and Ephemeral Streams: Ecology and Management, edited by T. Datry, N. Bonada, and A. J. Boulton, 1–20. London: Academic Press.

Deal, E., J. G. Venditti, S. J. Benavides, et al. 2023. "Grain Shape Effects in Bed Load Sediment Transport." *Nature* 613: 298–302. https://doi.org/10.1038/s41586-022-05564-6.

Giannopoulos, G., M. J. Sullivan, K. R. Hartop, et al. 2017. "Tuning the Modular Paracoccus Denitrificans Respirome to Adapt from Aerobic Respiration to Anaerobic Denitrification." *Environmental Microbiology* 19: 4953–4964. https://doi.org/10.1111/1462-2920.13974.

Gómez-Gener, L., G. Rocher-Ros, T. Battin, et al. 2021. "Global Carbon Dioxide Efflux from Rivers Enhanced by High Nocturnal Emissions." *Nature Geoscience* 14: 289–294. https://doi.org/10.1038/s41561-021-00722-3.

Gómez-Gener, L., A. R. Siebers, M. I. Arce, et al. 2021. "Towards an Improved Understanding of Biogeochemical Processes across Surface-Groundwater Interactions in Intermittent Rivers and Ephemeral Streams." *Earth-Science Reviews* 220: 103724. https://doi.org/10.1016/j.earscirev.2021.103724.

Groffman, P. M., K. Butterbach-Bahl, R. W. Fulweiler, et al. 2009. "Challenges to Incorporating Spatially and Temporally Explicit Phenomena (Hotspots and Hot Moments) in Denitrification Models." *Biogeochemistry* 93: 49–77. https://doi.org/10.1007/s10533-008-9277-5.

Higashino, M., J. J. Clark, and H. G. Stefan. 2009. "Pore Water Flow Due to near-Bed Turbulence and Associated Solute Transfer in a Stream or Lake Sediment Bed." *Water Resources Research* 45: W12414. https://doi.org/10.1029/2008WR007374.

Higashino, M., and H. G. Stefan. 2008. "Near-Bed Turbulence Models: Significance for Diffusional Mass Transfer at the Sediment/Water Interface." *Journal of Hydraulic Research* 46: 291–300. https://doi.org/10.3826/jhr.2008.2769.

Hotchkiss, E. R., and T. Del Sontro. 2023. "Organic Carbon Cycling and Ecosystem Metabolism." In Wetzel's Limnology, edited by J. P. Smol and I. Jones, 939–997. Amsterdam: Academic Press.

Ji, Q., A. E. Santoro, K. L. Casciotti, and C. Buchwald. 2015. "Nitrous Oxide Production by Nitrification and Denitrification in the Eastern Tropical South Pacific Oxygen Minimum Zone." *Global Biogeochemical Cycles* 42: 755–764. https://doi.org/10.1002/2015GL066853.

Koschorreck, M., K. H. Knorr, and L. Teichert. 2022. "Temporal Patterns and Drivers of CO_2 Emission from Dry Sediments in a Groyne Field of a Large River." *Biogeosciences* 19: 5221–5236. https://doi.org/10.5194/bg-19-5221-2022.

Larned, S. T., T. Datry, D. B. Arscott, and K. Tockner. 2010. "Emerging Concepts in Temporary-River Ecology." *Freshwater Biology* 55: 717–738. https://doi.org/10.1111/j.1365-2427.2009.02322.x.

Lauerwald, R., G. H. Allen, B. R. Deemer, et al. 2023. "Inland Water Greenhouse Gas Budgets for RECCAP2: 1. State-of-the-Art of Global Scale Assessments." *Global Biogeochemical Cycles* 37: e2022GB007657. https://doi.org/10.1029/2022GB007657.

Lipschultz, F., O. C. Zafiriou, S. C. Wofsy, M. B. McElroy, F. W. Valois, and S. W. Watson. 1981. "Production of NO and N_2O by Soil Nitrifying Bacteria." *Nature* 294: 641–643. https://doi.org/10.1038/294641a0.

López-Rojo, N., T. Datry, F. J. Peñas, et al. 2024. "Carbon Emissions from Inland Waters May be Underestimated: Evidence from European River Networks Fragmented by Drying." *Limnology and Oceanography Letters* 9: 553–562. https://doi.org/10.1002/lol2.10408.

Mackenthun, A. A., and H. G. Stefan. 1998. "Effect of Flow Velocity on Sediment Oxygen Demand: Experiments." *Journal of Environmental Engineering* 124: 222–230. https://doi.org/10.1061/(ASCE)0733-9372(1998)124:3(222).

McClain, M. E., E. W. Boyer, C. L. Dent, et al. 2003. "Biogeochemical Hot Spots and Hot Moments at the Interface of

Terrestrial and Aquatic Ecosystems." *Ecosystems* 6: 301–312. https://www.jstor.org/stable/3659030, https://doi.org/10.1007/s10021-003-0161-9.

Mendoza-Lera, C., A. Frossard, M. Knie, L. L. Federlein, M. O. Gessner, and M. Mutz. 2017. "Importance of Advective Mass Transfer and Sediment Surface Area for Streambed Microbial Communities." *Freshwater Biology* 62: 133–145. https://doi.org/10.1111/fwb.12856.

Mendoza-Lera, C., J. Löwer, and L. Rovelli. 2025. "Controls of Methane Oxidation in Dry Streambeds." *Limnetica* 45: 45–57. https://doi.org/10.23818/limn.45.12.

Messager, M. L., B. Lehner, G. Grill, I. Nedeva, and O. Schmitt. 2021. "Global Prevalence of Non-perennial Rivers and Streams." *Nature* 594: 391–397. https://doi.org/10.1038/s41586-021-03565-5.

Murphy, J., and J. P. Riley. 1962. "A Modified Single Solution Method for the Determination of Phosphate in Natural Waters." *Analytica Chimica Acta* 27: 31–36. https://doi.org/10.1016/S0003-2670(00)88444-5.

Oprei, A., J. Schreckinger, I. Franzmann, H. Lee, M. Mutz, and U. Risse-Buhl. 2024. "Light over Mechanics: Microbial Community Structure and Activity in Simulated Migrating Bedforms Are Controlled by Oscillating Light Rather than by Mechanical Forces." *FEMS Microbiology Ecology* 100: fiae073. https://doi.org/10.1093/femsec/fiae073.

Oprei, A., J. Schreckinger, T. Kholiavko, A. Frossard, M. Mutz, and U. Risse-Buhl. 2023. "Long-Term Functional Recovery and Associated Microbial Community Structure after Sediment Drying and Bedform Migration." *Frontiers in Ecology and Evolution* 11: 1112519. https://doi.org/10.3389/fevo.2023.1112519.

Paranaíba, J. R., R. Aben, N. Barros, et al. 2022. "Cross-Continental Importance of CH_4 Emissions from Dry Inland-Waters." *Science of the Total Environment* 814: 151925. https://doi.org/10.1016/j.scitotenv.2021.151925.

Quick, A. M., E. V. Arntzen, D. J. Martin, et al. 2019. "Nitrous Oxide from Streams and Rivers: A Review of Primary Biogeochemical Pathways and Environmental Variables." *Earth-Science Reviews* 191: 224–262. https://doi.org/10.1016/j.earscirev.2019.02.021.

Rocher-Ros, G., E. H. Stanley, L. C. Loken, et al. 2023. "Global Methane Emissions from Rivers and Streams." *Nature* 621: 530–535. https://doi.org/10.1038/s41586-023-06344-6.

Romaní, A. M., S. Amalfitano, S. Fazi, et al. 2017. "The Biota of Intermittent Rivers and Ephemeral Streams: Prokaryotes, Fungi, and Protozoans." In Intermittent Rivers and Ephemeral Streams: Ecology and Management, edited by T. Datry, N. Bonada, and A. J. Boulton. London: Academic Press.

Ryo, M., C. A. Aguilar-Trigueros, L. Pinek, L. A. H. Muller, and M. C. Rillig. 2019. "Basic Principles of Temporal Dynamics." *Trends in Ecology & Evolution* 34: 723–733. https://doi.org/10.1016/j.tree.2019.03.007.

Rysgaard, S., N. Risgaard-Petersen, and N. P. Sloth. 1996. "Nitrification, Denitrification, and Nitrate Ammonification in Sediments of Two Coastal Lagoons in Southern France." *Hydrobiologia* 329: 133–141. https://doi.org/10.1007/BF00034553.

Sander, R. 2015. "Compilation of Henry's Law Constants (Version 4.0) for Water as Solvent." *Atmospheric Chemistry and Physics* 15: 4399–4981. https://doi.org/10.5194/acp-15-4399-2015.

Scheidweiler, D., C. Mendoza-Lera, M. Mutz, and U. Risse-Buhl. 2021. "Overlooked Implication of Sediment Transport at Low Flow: Migrating Ripples Modulate Streambed Phototrophic and Heterotrophic Microbial Activity." *Water Resources Research* 57: e2020WR027988. https://doi.org/10.1029/2020WR027988.

Schreckinger, J., M. Mutz, and C. Mendoza-Lera. 2022. "When Water Returns: Drying History Shapes Respiration and Nutrients of Intermittent River Sediment." *Science of the Total Environment* 838: 155950. https://doi.org/10.1016/j.scitotenv.2022.155950.

Schulz, H., Y. Teitelbaum, J. Lewandowski, G. A. Singer, and S. Arnon. 2023. "Moving Bedforms Control CO_2 Production and Distribution in Sandy River Sediments." *Journal of Geophysical Research: Biogeosciences* 128: e2022JG007156. https://doi.org/10.1029/2022JG007156.

Silverthorn, S., D. Johnson, and H. Lee. 2024. "The Importance of Ditches and Canals in Global Inland Water CO_2 and N_2O Emissions." *Global Change Biology* 31: e70079. https://doi.org/10.1111/gcb.70079.

Skoulikidis, N., and Y. Amaxidis. 2009. "Origin and Dynamics of Dissolved and Particulate Nutrients in a Minimally Disturbed Mediterranean River with Intermittent Flow." *Journal of Hydrology* 373: 218–229. https://doi.org/10.1016/j.jhydrol.2009.04.032.

Skoulikidis, N. T., S. Sabater, T. Datry, et al. 2017. "Non-perennial Mediterranean Rivers in Europe: Status, Pressures, and Challenges for Research and Management." *Science of the Total Environment* 577: 1–18. https://doi.org/10.1016/j.scitotenv.2016.10.147.

Strauss, E. A., and G. A. Lamberti. 2000. "Regulation of Nitrification in Aquatic Sediments by Organic Carbon." *Limnology and Oceanography* 45: 1854–1859. https://doi.org/10.4319/lo.2000.45.8.1854.

Triska, F. J., J. H. Duff, and R. J. Avanzino. 1990. "Influence of Exchange Flow between the Channel and Hyporheic Zone on Nitrate Production in a Small Mountain Stream." *Canadian Journal of Fisheries and Aquatic Sciences* 47: 2099–2111. https://doi.org/10.1139/f90-235.

Van den Berg, J. H. 1987. "Bedform Migration and Bed-Load Transport in some Rivers and Tidal Environments." *Sedimentology* 34: 681–698. https://doi.org/10.1111/j.1365-3091.1987.tb00794.x.

von Schiller, D., S. Bernal, C. N. Dahm, and E. Martí. 2017. "Nutrient and Organic Matter Dynamics in Intermittent Rivers and Ephemeral Streams." In Intermittent Rivers and Ephemeral Streams: Ecology and Management, edited by T.

Datry, N. Bonada, and A. J. Boulton, 135–160. London: Academic Press.

von Schiller, D., T. Datry, R. Corti, et al. 2019. "Sediment Respiration Pulses in Intermittent Rivers and Ephemeral Streams." *Biogeosciences Discussions* 33: 1251–1263. https://doi.org/10.1029/2019GB006276.

Weber, G., and J. Kubiniok. 2022. "Spring Waters as an Indicator of Nitrate and Pesticide Pollution of Rural Watercourses from Nonpoint Sources: Results of Repeated Monitoring Campaigns since the Early 2000s in the Low Mountain Landscape of Saarland, Germany." *Environmental Sciences Europe* 34. https://doi.org/10.1186/s12302-022-00632-0.

Wood, S. N. 2017. Generalized Additive Models: An Introduction with R. Second ed. USA: Chapman and Hall/CRC. https://doi.org/10.1201/9781315370279.

Wrage, N., G. L. Velthof, M. L. van Beusichem, and O. Oenema. 2001. "Role of Nitrifier Denitrification in the Production of Nitrous Oxide." *Soil Biology and Biochemistry* 33: 1723–1732. https://doi.org/10.1016/S0038-0717(01)00096-7.

Zarnetske, J. P., R. Haggerty, S. M. Wondzell, and M. A. Baker. 2011. "Labile Dissolved Organic Carbon Supply Limits Hyporheic Denitrification." *Journal of Geophysical Research* 116: G04036. https://doi.org/10.1029/2011JG001730.

Zlatanović, S., J. Fabian, C. Mendoza-Lera, K. B. Woodward, K. Premke, and M. Mutz. 2017. "Periodic Sediment Shift in Migrating Ripples Influences Benthic Microbial Activity." *Water Resources Research* 53: 4741–4755. https://doi.org/10.1002/2017WR020656.

Supporting Information

Additional Supporting Information may be found in the online version of this article.

Submitted 16 October 2025
Revised 01 April 2026
Accepted 02 July 2026